ISBN: 978-3-95450-217-2 doi:10.18429/JACoW-ERL2019-WECOXBS03

BENCH TEST RESULTS OF CW 100 mA ELECTRON RF GUN FOR NOVOSIBIRSK ERL BASED FEL *

V. N. Volkov †, V. Arbuzov, E. Kenzhebulatov, E. Kolobanov, A. Kondakov, E. Kozyrev, S. Krutikhin, I. Kuptsov, G. Kurkin, S. Motygin, A. Murasev, V. Ovchar, V.M. Petrov, A. Pilan, V. Repkov, M. Scheglov, I. Sedlyarov, S. Serednyakov, O. Shevchenko, S. Tararyshkin, A. Tribendis, N. Vinokurov, BINP SB RAS, Novosibirsk, Russia

Abstract

Continuous wave (CW) 100 mA electron rf gun for injecting the high-quality 300-400 keV electron beam in Novosibirsk Energy Recovery Linac (ERL) and driving Free Electron Laser (FEL) was developed, built, and commissioned at BINP SB RAS. The RF gun consists of normal conducting 90 MHz rf cavity with a gridded thermionic cathode unit. Bench tests of rf gun is confirmed good results in strict accordance with our numerical calculations. The gun was tested up to the design specifications at a test bench that includes a diagnostics beam line. The rf gun stand testing showed reliable work, unpretentious for vacuum conditions and stable in long-term operation. The design features of different components of the rf gun are presented. Preparation and commissioning experience is discussed. The latest bench test beam results are reported.

INTRODUCTION

Recent projects of advanced sources of electromagnetic radiation [1] are based on the new class of electron accelerators where the beam current is not limited by the power of rf system – energy recovery linacs (ERLs). Such accelerators require electron guns operating in continuous wave (cw) mode with high average current. The only solution is an rf gun, where the cathode is installed inside the rf cavity. There are no back bombardment ions in rf guns so there are no cathode degradation, and the vacuum condition does not critical there (see Table 1). The most powerful Novosibirsk FEL [2] can be more powerful by one order on magnitude with this rf gun [3-5].

RF GUN AND DIAGNOSTIC STAND

The rf gun and diagnostic stand are presented in Fig. 1.

The RF gun cavity is made on the base of standard bimetallic cavity of Novosibirsk ERL. Detailed information can be found in [3-5]. Only the insert with the thermionic cathode-grid unit is built into the cavity. The gridded thermionic dispenser cathode is driven by special modulator with GaN rf transistor. The modulator generates a launch pulse voltage of up to 150 V and the duration of about 1 ns in any series with repetition frequencies of 0.01 - 90 MHz.

The insert focusing electrode has a concave form to decrease the electric RF field at the grid surface down to 1 MV/m (by one order on magnitude). Due to this the fields before the grid and after it becomes equal to each other so the laminarity of the electron beam flow through the grid remains higher and beam emittance lower. Furthermore, the insert focusing electrode executes the strong rf focusing on the beam just near the cathode that ensures the beam emittance compensation at the relatively low electric field at the cathode. Also it ensures the absence of dark currents in the beam.

There are in the stand: 30 kW water cooled beam dump with 5 cm lead radiation shield, wideband Wall Current Monitor (WCM2) inserted into the replaceable target, Transition Radiation Sensor, the pair of standard WCM, three focusing solenoids, and the special testing cavity.

Table 1: Measured RF Gun Characteristics

Average beam current, mA	≤100
Cavity Frequency, MHz	90
Bunch energy, keV	100 ÷ 400
Bunch duration (FWHM), ns	0.06 ÷ 0.6
Bunch emittance, mm mrad	10
Bunch charge, nC	0.3 ÷ 1.12
Repetition frequency, MHz	0.01 ÷ 90
Radiation Doze Power, mR/h	100/2m
Operating pressure, Torr	10^{-9}…10^{-7}
Cavity RF loses, kW	20

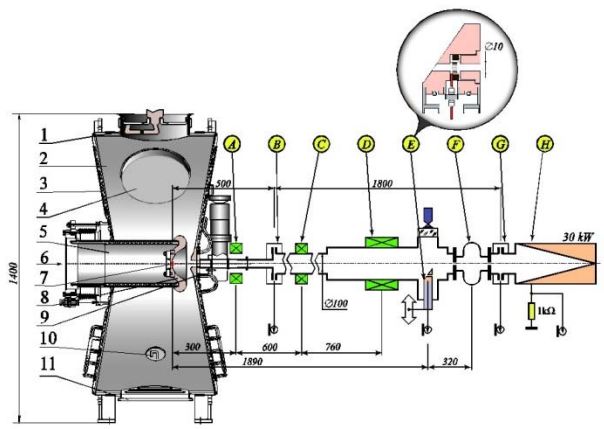

Figure 1: Rf gun and stand layout: 1-Power input coupler; 2- Cavity shell; 3-Cavity back wall; 4-Sliding tuner; 5-Insert; 6-Cathode injection/extraction channel; 7-Thermionic cathode-grid unit; 8-Concave focusing electrode; 9-Cone like nose; 10-Loop coupler; 11-Vacuum pumping port; A-Emittance compensation solenoid; B-First Wall Current Monitor (WCM); C, D - Solenoids ; E-Wideband WCM and transition radiation

* Work supported by Russian Science Found- n (project N 14-50-00080)
† v.n.volkov@inp.nsk.su

ISBN: 978-3-95450-217-2 doi:10.18429/JACoW-ERL2019-WECOXBS03

target; F – Test Cavity; G-third WCM; H-Faraday cup and Water-cooled beam dump.

BENCH TESTING RESULTS

Beam Current Regulation

There is the problem of thermionic dispenser cathodes that the thermionic current emission ability depends on the emission current. This is demonstrated in Figure 2 where the beam current from the cathode is increased due to increasing of repetition frequency. To preserve the bunch charge to be stable we have to change the bias voltage (V_{bias}) also if the launch pulse voltage (V_{launch}) is stable.

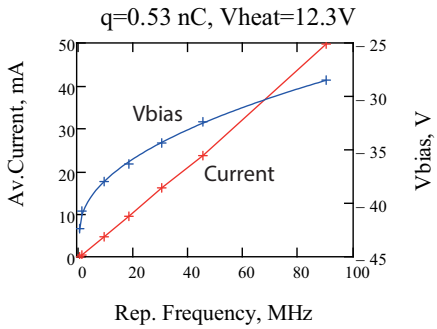

Figure 2: Beam current rising due to repetition frequency increasing (V_{launch}=*100 V*).

There are some methods of beam current increasing: decreasing of the grid bias voltage (V_{bias}), increasing of the modulator pulse voltage (V_{puls}), and increasing of the repetition frequency. Also there must be increased the cathode heating voltage (V_{heat}) to compensate the cathode emission ability derating. The applying of these methods is demonstrated in Fig.3.

In the beginning of the operation with the large beam current of 100 mA there have made the processing procedure. A rising the beam current by 10-20 mA steps in each day was made during one week to normalize the vacuum condition in the beam dump. It is interesting that the deteriorated vacuum condition after the each step was being low during all day without changing but in the next day we can make a new current increasing step while the vacuum deteriorates down to the previous level.

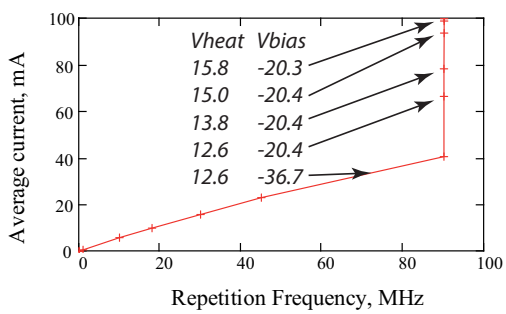

Figure 3: Typical method current rising (V_{launch}=*120V*).

Calibration of Cavity Voltage Meter

To measure the beam energy there is used the measuring of time delay between two wall current monitors. Since the particle velocities at the relatively low energy are lower than speed of light. It is demonstrated in Fig.4 where the measured data are fitted by the theory curve obtained from relativistic equations. This effect was used for the calibration of the cavity voltage meter. The calibration has a high accuracy not more than 1 %. There have to take into account that bunch energy also differ from the cavity voltage of about -1… -1.3 % in the range of 100-400 keV energies.

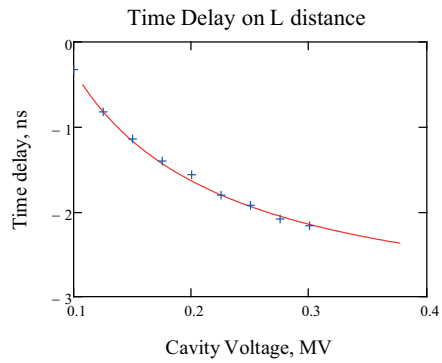

Figure 4: Measured data fitting by theory curve.

Cavity Testing up to 400 kV

To test the cavity for a high voltage the cavity voltage was increased with step by step method. After each step there required 1/2 an hour to normalize the vacuum condition (see Fig. 5).

Maximum beam current at 400 kV (see Fig. 6) was being limited by the beam dump permissible power and deteriorating of vacuum condition in it that requires some days to normalize the vacuum condition.

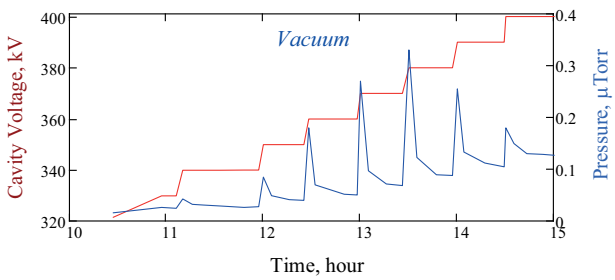

Figure 5: Cavity testing process behavior.

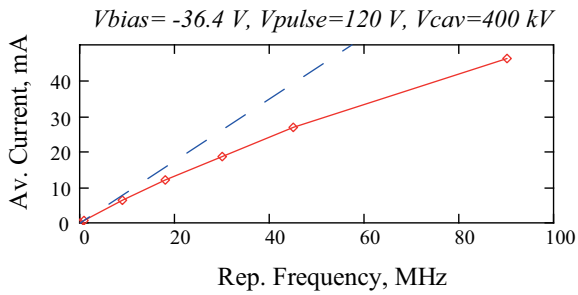

Figure 6: Beam current testing at 400 kV cavity voltages.

ISBN: 978-3-95450-217-2 doi:10.18429/JACoW-ERL2019-WECOXBS03

Launch Phase Functions

Energy distribution along the bunch is changed due to the launch phase changing. The energy of head particles becomes lower than the tail one at lower launch phases as shown in Fig. 7. The minimal launch phase value of 31° is limited by the duration of the launch pulse of 1 ns. At launch phases of more than 120° there are appeared back accelerated electrons that can corrupt the cathode quality.

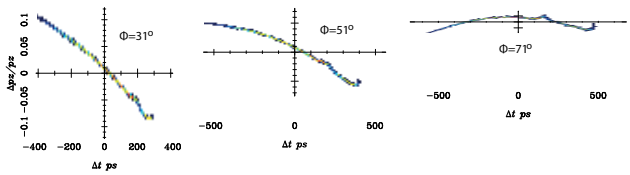

Figure 7: Energy distributions of particles along the bunch just after the rf gun for different launch phases.

Also there is changed the bunch energy as it shown in Fig. 8. The maximal bunch particle energy is at 68°, and minimal bunch length at 31°. It is used for velocity bunching on a drift space and for the phase instability (jitter) compensation.

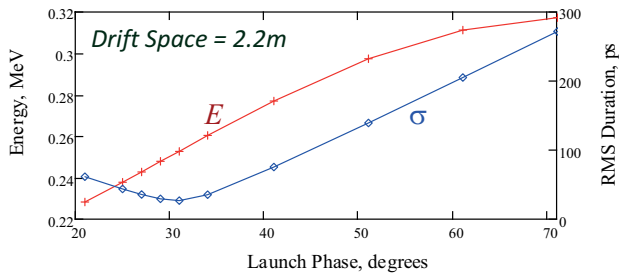

Figure 8: Launch phase functions.

Direct Bunch Length Measurement

There are complex particle distributions along the bunch due to plasma oscillation into a cathode-grid unit. On the drift space this distribution are changed significantly. The example of this at the launch phase of 31° is shown in Fig. 9. Current distributions along the bunch are shown for those coordinates where wall current monitors are placed in the stand. Frontal spike is formed into cathode-grid gap of 80 micron length. Then it grows and becomes short of about 20 ps FWHM while traveling along the drift space.

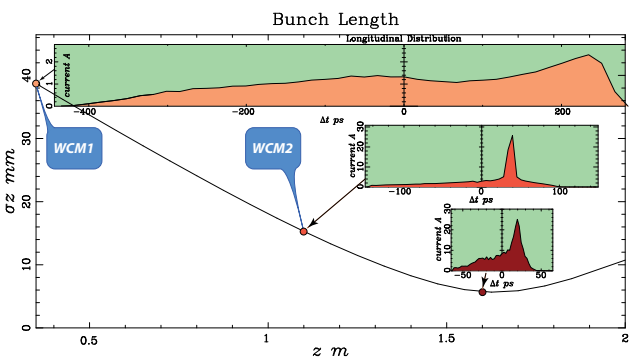

Figure 9: Bunch duration behaviour on the drift space.

The direct measurements of these distributions are difficult because the frequency bend of our 6 m coaxial lines with our 4 GHz oscilloscope are limited. Only measured values of more than 200 ps are possible in this configuration (see Fig.10). But we have found another method to determine the unique particle distribution and the bunch length with help of a special test cavity. This method will be described in the next chapter.

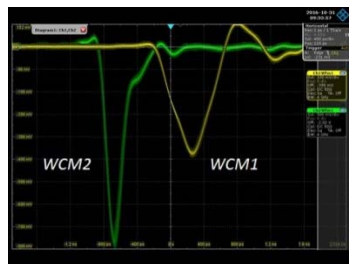

Figure 10: Measured bunch distributions by oscilloscope.

Cathode-Grid Plasma Oscillation Effect

Calculations and experiments have shown the plasma oscillation effect into the cathode grid gup of 80 microns depends on the cathode emission ability. That is demonstrated in Fig. 11 where the amount of frontal spikes due to the emission ability increasing is enlarged.

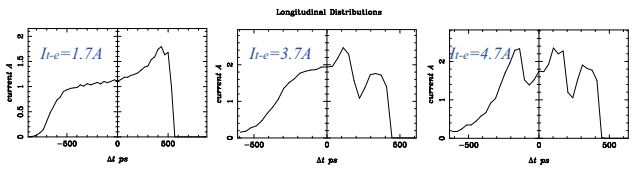

Figure 11: The enlarging of frontal spike amounts in bunch current distributions due to increasing of cathode emission ability ($I_{t\text{-}e}$).

This effect can be explained as follows. There are known that cathode current of endless beam is limited by the beam space charge according to “law of 3/2”. Before the launch pulse comes to the cathode the cathode grid gup is empty so for the frontal particles that appeared after the pulse has been come this law does not work and the beam current is large in view of the spike that is limited only by the cathode emission ability and by the frontal slope of the launch pulse. So due to beam plasma oscillation some amount of current spikes is appeared in the current distribution.

For a low emission ability the bunch at the end of the drift space becomes having two parts unlike to the bunch comes with large emission as shown in Fig. 12. The excitation of a testing cavity by such a double bunch will be having anomalous behaviour due to interfere effect between these parts. ^

ISBN: 978-3-95450-217-2 doi:10.18429/JACoW-ERL2019-WECOXBS03

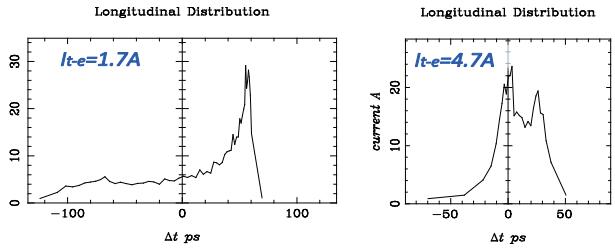

Figure 12: Particle distributions transformed to the drift space end.

Numerical modeling of the excitation and experiments are made with a special cavity having the main mode frequency of 1.4 GHz. In the frequency bend of up to 4 GHz for our oscilloscope there are many HOMs in the cavity. But only two of them (3674 and 4046 MHz) have enough coupling impedances with the beam and with pickups.

The simulated excitation amplitudes of these HOMs by bunch of Fig.11 depending on the launch phase are shown in the upper of Fig. 13. We see the shorter bunch length the large excitation amplitudes. Only the excitation with low emission bunch have the anomalous excitation behaviour due to the interfere effect. The same effect is observed in the experiments shown at the bottom of Fig. 13 where the emission ability was regulated by changing of cathode heating voltage.

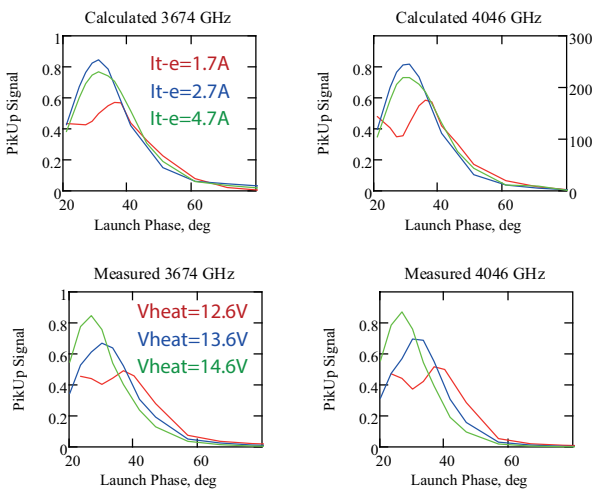

Figure 13: Excitations of test cavity HOMs. Calculations (at the top) and experiment (at the bottom) shows the interference for the low cathode emission bunches.

So we can conclude the numerical simulation of beam dynamics in cathode grid units [4] has enough accuracy to describe beam behaviors and to determine the minimal bunch rms length in the RF gun as 20 ps.

Launch Phase Jitter Compensation

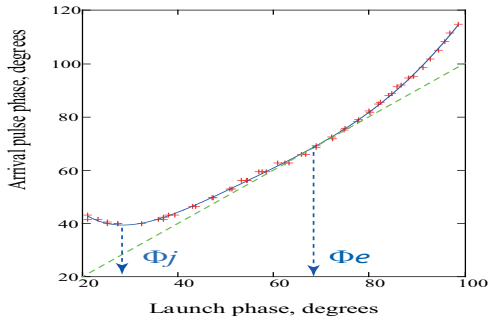

Figure 14: Arrival pulse phase behavior.

The jitter compensation effect has measured between two WCMs with 1.2 m distance between them (see Fig. 14). At the launch phase of 27 degrees the arrival time is independent on launch phase so the jitter is compensated there. I.e. the requirement to the phase stability of the modulator pulses is not high at the launch phase of 27°.

Emittance Measurements

Bunch emittance was measured by solenoid focusing method when the spot size of the beam focussed to a target is measured through CCD camera registering the transition radiation.

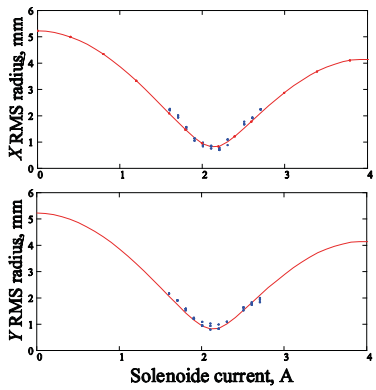

Figure 15: Measured and calculated beam behaviors.

The measured data behaviour on the focusing solenoid strength confirms to ASTRA [6] numerically calculated behaviour (see Fig. 15) with the accuracy of 9%. It corresponds to beam emittance of 15 mm mrad. As simulation shows the emittance can be compensated by proper focusing down to 10 mm mrad.

Dark and Leakage Particle Contaminations

Two spots in the RF gun cavity with peak surface field of 10-14 MV/m are the sources of field emitted dark currents (see Fig. 16). There are no dark currents in the beam since dark current trajectories are far from the beam.

ISBN: 978-3-95450-217-2 doi:10.18429/JACoW-ERL2019-WECOXBS03

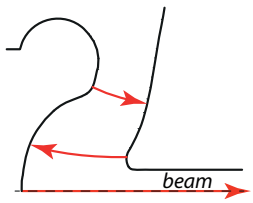

Figure 16: Dark current trajectories in the RF gun cavity.

The leakage current may be appeared in the cathode grid unit under the field of the cavity percolated through the grid. Dependencies of this current on the bias voltage and on the heating voltage are shown in Fig. 17. So to exclude the leakage current from the beam we have to choose the proper bias voltage.

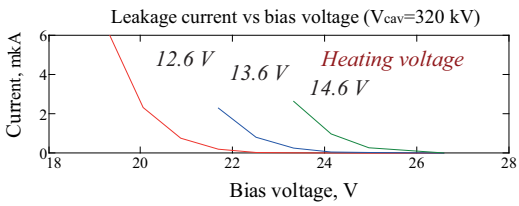

Figure 17: Leakage current from the cathode grid unit.

Radiation Background

The source of bremsstrahlung radiation is the field emission current described by Fouler-Nordheim equation

$$I \approx (\beta E)^{2.5} exp\left(-\frac{B\varphi^{1.5}}{\beta E}\right) \quad (1)$$

Radiation background was measured behind the cavity wall with the thickness of 15 mm. The enhancement factor measured is found to be β=628 for one of sensors (see Fig. 18, red line).

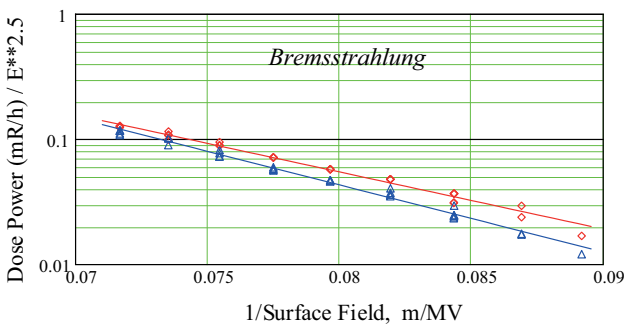

Figure 18: Measured radiation background by two different sensors in different places of the stand.

It was used as the base for simulation of enhancement factors for different shield thickness (10, 5, 3 mm), for bremsstrahlung power, for field emission particle power, and for field emission current (see Fig. 19). The enhancement factor for emission current is found to be β_I=1250 (see Table 2). For the comparison, it is large by one order on magnitude than enhancement factors of superconducting cavities preparing with a perfect modern technology.

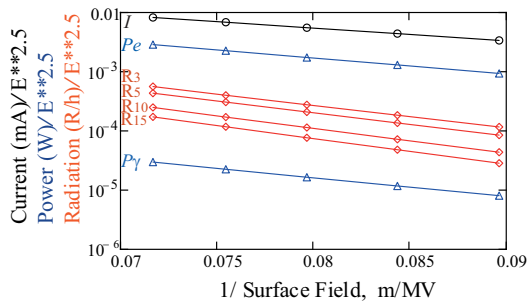

Figure 19: Calculated and measured (R15) field emission process.

Table 2: Simulated Enhancement Factors for Different Parameters of the Radiation Process in the RF Gun

Name		label	β
Dark Current of Field Emission		I	1264
Dark Current Power		Pe	1003
Bremsstrahlung Power		Pγ	865
Cu Shielded Dose Power	d=3 mm	R3	721
	d=5 mm	R5	695
	d=10mm	R10	649
	d=15mm	R15	628

There is interesting that all parameters in the radiation process are confirmed to F-N equation and have different enhancement factors.

REFERENCES

[1] N. A. Vinokurov and E. B. Levichev, "Undulators and wigglers for the production of radiation and other applications", Physics-Uspekhi, 58, 2015, pp. 850–871. doi: 10.3367/UFNe.0185.201509b.0917

[2] G. N. Kulipanov *et al.*, "Novosibirsk Free Electron Laser—Facility Description and Recent Experiments", IEEE TRANSACTIONS ON TERAHERTZ SCIENCE AND TECHNOLOGY, 5, doi:10.1109/ TTHZ.2015.2453121.

[3] V.N. Volkov *et al.*, "First test results of RF gun for the Race-Track Microtron Recuperator of BINP SB RAS" in *Proc. RuPAC'12*, Saint-Petersburg, Russia, 2012. paper:TUPPB049

[4] V. Volkov *et al.*, "Thermionic cathode-grid assembly simulations for rf guns", in *Proc. PAC'09*, Vancouver, Canada, 2009. paper:MO6RFP087

[5] V. Volkov *et al.*, "Thermocathode Radio-Frequency Gun for the Budker Institute of Nuclear Physics Free-Electron Laser", ISSN 1547-4771, Physics of Particles and Nuclei Letters, Vol. 13, No. 7, 2016, pp. 827–830. doi:10.1134/S1547477116070517

[6] K. Floettmann, ASTRA User`s Manual, http://www.desy.de~mpyflo/Astra_docomentation.